QUT

QUTePrints
Open-access archive of QUT research literature

COVER SHEET

This is the authors pre-print version that is accessed from:

Mallet, D.G. and Pettet, G.J. (2006) A Mathematical Model of Integrin-Mediated Haptotactic Cell Migration. *Bulletin of Mathematical Biology* **68(2):pp. 231-253.**

Accessed from   http://eprints.qut.edu.au

A Mathematical Model of Integrin–Mediated Haptotactic Cell Migration

D.G. Mallet [a],* G.J. Pettet [a]

[a]*School of Mathematical Sciences, Queensland University of Technology, Brisbane, Australia.* [1]

Abstract

Haptotactic cell migration, a directed response to gradients of cell–extracellular matrix adhesion, is an important process in a number of biological phenomena such as wound healing and tumour cell invasion. Previously, mathematical models of haptotaxis have been developed on the premise that cells migrate in response to gradients in the density of the extracellular matrix. In this paper we develop a novel mathematical model of haptotaxis which includes the adhesion receptors known as integrins and a description of their functional activation, local recruitment and protrusion as part of lamellipodia. Through the inclusion of integrins, the modelled cell matter is able to respond to a true gradient of cell–matrix adhesion, represented by functionally active integrins. We also show that previous matrix–mediated models are in fact a subset of the novel integrin–mediated models, characterised by specific choices of diffusion and haptotaxis coefficients in their model equations. Numerical solutions suggest the existence of travelling waves of cell migration that are confirmed via a phase plane analysis of a simplified model.

Key words: haptotaxis, cell migration, integrin, travelling waves, wall of singularities

1 Introduction

Cell migration is at the root of processes such as wound healing angiogenesis and tumour cell invasion. Migration can be driven by numerous factors

---

* Corresponding author.

   Email address: `dg.mallet@qut.edu.au` (D.G. Mallet).

[1] Mailing Address: GPO Box 2434, Brisbane, QLD 4001, Australia. Fax Number: +61 7 3864 2310.

including the directed response to gradients in pressure, chemical substances and components of the extracellular matrix (ECM).

Of particular interest to this work is the process of tumour or normal cell invasion into extracellular matrix, as a comprehensive understanding of this phenomenon can be important in the development of novel tissue engineering and tumour treatment strategies. Haptotactic migration, being the directed motion of cells due to gradients in bound or insoluble chemicals (in the case of cell invasion, gradients in bound cell–ECM adhesion molecules), is therefore of great importance in cell invasion.

Previous modelling of haptotactic migration of cells has favoured two main types of mathematical model. *Cell population* models with haptotactic migration have developed from the more commonly modelled cell migration phenomenon of chemotaxis (the directed migration of cells due to gradients in soluble chemical attractants), while models of *individual cell* migration have arisen from models of cell adhesion to ligands in the underlying substrate. These two types of model are discussed below.

The models of haptotactic migration of cell populations can be broadly grouped into two classes: mass conservation and mechano–chemical models. Maini (1989) developed a mechano–chemical model to investigate the generation of one dimensional spatial and spatio–temporal patterns. This model included mass balance equations for the conservation of cells and extracellular matrix, along with a mechanical force balance equation. While the application of Maini's work is of limited interest here, the model itself is one of the earliest references to a mathematical model of haptotaxis in a population of cells. Furthermore, the model employs a cell velocity which is proportional to the gradient of the ECM density. We note that Murray (1993) and Tracqui (1995) developed similar models of mechano–chemical nature, with Murray including a long range sensor of ECM gradients in the cell flux. All of these models neglect the underlying mechanisms of cell–ECM adhesion in their descriptions of haptotactic migration, favouring a simple relationship to the ECM density gradient for describing haptotaxis.

Perumpanani and Byrne (1999), Perumpanani *et al.* (1996, 1999) Anderson and Chaplain (1998); Anderson *et al.* (2000) and Marchant (1999) also developed models for cell population migration which relied solely on mass balance equations. These models again utilised a cell velocity proportional to the gradient in ECM density, and in particular the collagen or fibronectin components of the ECM. Anderson and Chaplain (1998) and Anderson *et al.* (2000) also developed discrete cell migration models that were derived from the mass balance models.

With regard to individual cell models, Lauffenburger (1989) and DiMilla *et al.*

(1991) model the distribution of adhesion receptors, cell–substratum adhesion and intracellular force generation of moving cells. These models use ordinary differential equations which introduce kinetic terms describing receptor activity in cell–adhesion based migration processes.

To date, there is a distinct lack of theoretical literature in the area of integrin–mediated haptotactic cell population migration which accurately models cell adhesion to the ECM – a fundamental process in haptotaxis.

Adhesion to the ECM is important for cell migration. Factors involved in cell–ECM adhesion include the particular cell line, ECM composition, the ECM degrading process of proteolysis, and the functionality of the cell's integrins (Aplin *et al.*, 1998). Cell–ECM adhesion also plays an important role in cell–ECM signalling which can modify cell dynamics, adhesion and death (Aplin *et al.*, 1998).

Integrins, a family of transmembrane glycoproteins, act as receptors for specific ligands that may be constituents of the ECM (Aplin *et al.*, 1998), effecting cell adhesion to the matrix. In defining haptotaxis, Carter (1965) stated that it was the movement of cells on an adhesion gradient, in the direction of increasing substrate adhesion. With the introduction of integrins, we model the haptotactic response of cells to gradients in insoluble ECM macromolecules through a response to gradients in functionally active integrins. These functionally active integrins represent locations of cell–ECM adhesion where the integrins are actively bound to ligands in the ECM. On the other hand, functionally inactive integrins are those which are simply present in the cell membrane and have no external attachments.

In this paper we develop a mathematical model which, through the inclusion of integrins, describes the underlying processes of cell–extracellular matrix adhesion which are essential in haptotactic cell migration and indeed cell survival. The model offers a theoretical framework with which to test hypotheses, explore experimental strategies and seek descriptions of behaviours that are outcomes of nonlinear interactions which may be difficult to manipulate experimentally. While the model is different from previous "ECM–mediated" haptotaxis models, it is possible to show a direct relationship between the two model types. We note that through the inclusion of integrins, it will be possible to investigate in the future, the phenomenon of anoikis, or apoptotic cell death due to incorrect or insufficient ECM attachment (Frisch and Ruoslahti, 1997), and the inhibition of haptotaxis through integrin–blocking.

In the following sections, we develop the new mathematical model of haptotaxis before conducting a nondimensionalisation and presenting numerical simulations of the model behaviour. Then we develop a simplification of the integrin–mediated model which identifies a limiting case relationship between

integrin–mediated and ECM–mediated haptotaxis models. A comparison of the full and simplified integrin–mediated models and an ECM–mediated model is presented with regard to the exhibited cell migration speeds. Finally, a further model simplification is presented that allows for a phase plane analysis which confirms the existence of travelling waves of cell migration.

2   Mathematical Model

The model proposed employs a mass conservation approach to determining the temporal and spatial behaviour of the five species deemed relevant in this examination of the process of cell migration. We begin by denoting $N(\mathbf{x}, t)$, $E(\mathbf{x}, t)$, $P(\mathbf{x}, t)$, $A(\mathbf{x}, t)$ and $I(\mathbf{x}, t)$ to be the density of cellular material, extracellular matrix density, protease concentration, and the densities of functionally active and functionally inactive integrins respectively. It should be noted that by *functionally inactive integrins*, we refer to those integrins which are simply present in the cell membrane and do not have any connection to ECM resident ligands. On the other hand, by *functionally active integrins*, we refer to those integrins which have formed a complex with an appropriate ECM resident ligand.

In the model presented here we describe both the active and inactive integrins as continua in space and time, in contrast to the concept of "bound receptors per cell", as employed by Sherratt *et al.* (1993) and MacArthur (2002) in their models of chemotactic and haptotactic cell migration. We now develop equations describing the evolution of both classes of integrins.

2.1   *Functionally Active and Inactive Integrins*

As defined above, functionally active integrins are those which are actively bound to the ligands of the extracellular matrix, and it is for this reason that we consider the active integrins to be immobile. In the locomotion of cells, a number of processes are observed which are common to most cell types (Maheshwari and Lauffenburger, 1998). These include membrane extension (lamellipod extension), formation of attachments, contractile force generation, cell detachment and front/rear asymmetry. Here, we model the formation of attachments through the interaction between inactive integrins and the extracellular matrix. Detachment of cells from the ECM is modelled through a term for natural decay of active integrins. Hence the kinetic terms for active integrin conservation are similar to those presented in Lauffenburger (1989) and DiMilla *et al.* (1991), and the conservation equation for active integrins

4

is given by

$$\frac{\partial A}{\partial t} = \underbrace{k_1 I E}_{\text{binding}} - \underbrace{k_2 A}_{\text{unbinding}}, \tag{1}$$

where k_1 and k_2 are the rate constants for attachment and detachment, respectively.

The dynamic interaction between active and inactive integrins is demonstrated through the attachment and detachment terms in the following equation, both of which are the same as those in equation (1), with reversed sign. Furthermore, new inactive integrins are created while the total density per unit volume of integrins is less than some maximum level. One of the novel aspects of this model is its description of lamellipod protrusion. To model the flux of unbound or inactive integrins caused by the extension of lamellipodia, we include a nonlinear diffusion term for the inactive integrin density. We take the nonlinear diffusion coefficient to be $D_I I$ for simplicity and note that other forms may be used. As the amount of cell matter in the protrusion is negligible compared with the great number of integrins contained therein, we assume that the coefficient of inactive integrin diffusion is much larger than that of cell matter. Furthermore, there is a contribution to the flux of inactive integrins due to the flux of the cells to which they are connected. This gives the following conservation equation for functionally inactive integrins

$$\frac{\partial I}{\partial t} = \underbrace{\nabla \cdot (D_I I \nabla I - D_c I \mathbf{v}_N)}_{\text{protrusion and convection}} - \underbrace{k_1 I E}_{\text{binding}} + \underbrace{k_2 A}_{\text{unbinding}} + \underbrace{\bar{k}_3 (\bar{k}_{20} N - A - I)}_{\text{creation}}, \tag{2}$$

where D_I is assumed to be constant, $\mathbf{v}_N$ is the as yet unspecified cell matter velocity at which the inactive integrins are convected as part of the cell membrane, with convection coefficient D_c. The parameter $\bar{k}_3$ is the constant rate of increase in the inactive integrins density per unit volume, and $\bar{k}_{20}$ represents the integrin–carrying capacity of cells.

Combining the detachment term, $k_2 A$, into the integrin production term in the above equation gives

$$\begin{aligned}
\frac{\partial I}{\partial t} =& \nabla \cdot (D_I I \nabla I - D_c I \mathbf{v}_N) - k_1 I E \\
&+ \bar{k}_3 \bar{k}_{20} \left(N + \left(\frac{k_2}{\bar{k}_3 \bar{k}_{20}} - \frac{1}{\bar{k}_{20}} \right) A - \frac{1}{\bar{k}_{20}} I \right).
\end{aligned} \tag{3}$$

Now, by assigning

$$k_3 = \overline{k}_3\,\overline{k}_{20}, \quad k_4 = \frac{k_2}{\overline{k}_3 \overline{k}_{20}} - \frac{1}{\overline{k}_{20}}, \quad k_5 = \frac{1}{\overline{k}_{20}},$$

equation (3) may be written as

$$\frac{\partial I}{\partial t} = \nabla \cdot (D_I I \nabla I - D_c I \mathbf{v}_N) - k_1 I E + k_3 \left(N + k_4 A - k_5 I \right), \tag{4}$$

where k_4 is related to the increase in the new inactive integrin production rate due to recruitment and endocytosis, or active integrin recycling, as well as the decrease in the production rate due to integrin crowding, and k_5 reflects the relative packing density of the unbound integrins per unit of cellular material.

In the above equation it should be noted that the constant k_4 may take on positive or negative values. Note also that if $k_4 > 0$, the presence of active integrins increases the possible inactive integrin density – this models endocytosis and also recruitment of new inactive integrins to points of cell–ECM adhesion.

Returning to the inactive integrin convection coefficient, D_c, we now explain the implications of its variation. Recall that in this model we consider I and N to be local densities (rather than volume fractions) of inactive integrins and cellular material. As such, the local density of inactive integrins may convect independently from the local density of cell matter, thus leading to values of $D_c < 1$. On the other hand, there is the possibility of perfectly efficient integrin convection, where we see convection of all inactive integrins which are connected to migrating cell matter. This would imply $D_c = 1$. Finally we note that $D_c > 1$ would imply that more than the available density of inactive integrins convects with migrating cells, and therefore this case is ignored.

2.2 Cell Matter, Extracellular Matrix and Protease

Coupled with the integrin equations are the three conservation equations for the densities of cellular material and extracellular matrix, and the protease concentration. We consider the density of cell matter at some point in space $\mathbf{x}$ to be dependent on cell migration, proliferation and death. As discussed earlier, we focus on haptotactic cell migration and small scale random cell motility, leading to a cell matter flux given by

$$\mathbf{J}_N = -D_N(\cdot)N\nabla N + \eta(\cdot)N\nabla A, \tag{5}$$

6

where $D_N(\cdot)$ is the diffusion coefficient, $\eta(\cdot)$ is the haptotactic coefficient, and $(\cdot)$ indicates the possibility that the coefficients may be functions of any of the independent and dependent variables. For the purposes of equation (4), this implies a cell velocity of

$$\mathbf{v}_N = -D_N(\cdot)\nabla N + \eta(\cdot)\nabla A. \tag{6}$$

Here we note one of the most important differences between this novel model and previous haptotaxis models. Previous models of haptotactic migration (for example Maini (1989), Tracqui (1995), Perumpanani *et al.* (1996), Anderson and Chaplain (1998) and Anderson *et al.* (2000)) have used a cell flux of the form

$$\mathbf{J}_N = k(\cdot)N\nabla E, \tag{7}$$

with $k(\cdot)$ used to represent the haptotactic coefficient function. This implies that the haptotactic response of cells is directed by the concentration gradient of the extracellular matrix. In most cases $k(\cdot)$ is taken to be constant and as such, these models essentially neglect any adhesion receptor (integrin) involvement.

The role of receptors in cell migration has been taken into account *implicitly* in some models of chemotaxis through the use of the *receptor–kinetic law* (Lauffenburger and Linderman, 1993) in the coefficient function of the active migration term (see for example, Sherratt (1994); Olsen *et al.* (1995, 1996)). Others have described mathematically, the role of receptors in chemotactic migration of amoebae in response to cAMP gradients (Hoefer *et al.*, 1995a,b; Othmer *et al.*, 2000). Dallon and Othmer also considered cell-to-cell signalling in relation to cAMP signals in Dictyostelium discoideum (Dallon and Othmer, 1997, 1998), although these models use quite different approaches from that used here. Both of these models consider the signalling process through intracellular and extracellular dynamics with quite interesting observations produced in Dallon and Othmer (1997) where a discrete-cell continuous-chemical approach is used.

Rather than including the effects of receptors or integrins into the coefficient of haptotactic migration as in the above models, here the integrin effects are incorporated through the response to the *gradient* in active integrins. In this way, rather than altering the magnitude of the haptotactic response, the integrins produce an explicit effect on the *direction* of motion. Given that haptotaxis is the phenomenon by which cells on an adhesion gradient are directed towards higher adhesion site concentrations, we consider the gradient of functionally active integrins to model the gradient of "recognised" adhesion sites. As such, the haptotactic response of cells is assumed to depend on the concentration

gradient of functionally active integrins. Hence, through the incorporation of functionally active integrins, the model presented in this paper allows for a more mechanically sound description of haptotaxis than ECM–mediated models.

Here, as in Perumpanani *et al.* (1999), proliferation of cells is assumed to occur in a logistic manner, bounded above by some maximum cell matter level k_7. Hence the conservation equation for cell matter is given by

$$\frac{\partial N}{\partial t} = \underbrace{\nabla \cdot (D_N(\cdot)N\nabla N}_{\text{diffusion}} - \underbrace{\eta(\cdot)N\nabla A)}_{\text{haptotaxis}} + \underbrace{k_6N(k_7 - N)}_{\text{proliferation}}, \tag{8}$$

where k_6 and k_7 are constants representing the rate of proliferation and maximum cell density, respectively.

Next, consider the density of the extracellular matrix. As the ECM is composed of a cross–linked network, or matrix, of proteins, its motility is negligible compared with the other species considered in this model. Hence, the ECM density varies due to degradation and production only. To allow cells to migrate, the matrix may be degraded to some extent by cell secreted proteolytic enzymes (proteases), in a tightly controlled process known as proteolysis (Stetler–Stevenson *et al.*, 1993). In itself, proteolysis is a complex process involving a sequence of events including (but not limited to) the secretion of the enzymes in inactive forms, and their subsequent activation. Here, as in Anderson *et al.* (2000) and Perumpanani *et al.* (1999), we adopt a simplified view of the process whereby proteolytic degradation is modelled by the product of the densities of protease and ECM representing the frequency of interaction between the same two species.

It is assumed that cells may produce ECM proportional to the level of cellular proliferation, in order to form a framework for migration and adhesion–mediated survival. Thus, the ECM conservation equation is

$$\frac{\partial E}{\partial t} = \underbrace{k_8N(k_7 - N)}_{\text{cellular secretion}} - \underbrace{k_9PE}_{\text{proteolysis}}, \tag{9}$$

where k_8 and k_9 are constants representing the rate of production of ECM by cells and the rate of proteolytic degradation, respectively.

Proteases are responsible for the depletion of the extracellular matrix that leads to the invasion of tumour cells into surrounding tissue. As protease molecules are small we assume that they diffuse naturally throughout the spatial domain. Furthermore, we consider only natural decay of protease. In past models, such as Anderson *et al.* (2000) and Perumpanani *et al.* (1999), it has been assumed that invasive cells secrete proteases to decay the ECM

either independently of ECM density or when they come in contact with the matrix. Here we adopt the strategy used by Perumpanani *et al.* (1999) and assume that the invasive cells secrete proteases when they come in contact with the ECM. Hence, the conservation equation for protease is given by

$$\frac{\partial P}{\partial t} = \underbrace{D_P \nabla^2 P}_{\text{diffusion}} + \underbrace{k_{10} N E}_{\text{production}} - \underbrace{k_{11} P}_{\text{natural decay}}, \tag{10}$$

where D_P is the constant coefficient of natural protease diffusion, k_{10} and k_{11} are constants representing the rate of production of protease and the rate of natural protease decay, respectively.

Hence, equations (1)–(10) form the model equations for integrin–mediated haptotactic cell migration and for clarity, the complete system is rewritten as

$$\begin{aligned}
\frac{\partial A}{\partial t} &= k_1 I E - k_2 A, \\
\frac{\partial I}{\partial t} &= \nabla \cdot (D_I I \nabla I + D_c D_N(\cdot) I \nabla N - D_c \eta(\cdot) I \nabla A) \\
&\qquad\qquad - k_1 I E + k_3 (N + k_4 A - k_5 I), \\
\frac{\partial N}{\partial t} &= \nabla \cdot (D_N(\cdot) N \nabla N - \eta(\cdot) N \nabla A) + k_6 N(k_7 - N), \\
\frac{\partial E}{\partial t} &= k_8 N(k_7 - N) - k_9 P E, \\
\frac{\partial P}{\partial t} &= D_P \nabla^2 P + k_{10} N E - k_{11} P.
\end{aligned} \tag{11}$$

We note that appropriate boundary and initial conditions are required for completion of the model and these are discussed in the following section.

3 Numerical Simulations

3.1 Nondimensionalisation

Here we consider the model equations (11) in a one dimensional spatial domain where $x \in [0, L]$, with L a constant domain length, and D_N and η are taken to be constants. We first introduce the dimensionless variables $A^*, I^*, N^*, E^*, P^*, x^*$ and t^*, and dimensioned constants $\hat{A}, \hat{I}, \hat{N}, \hat{E}, \hat{P}, \hat{X}$, and τ, such that

$$A^* = \frac{A}{\hat{A}}, \quad I^* = \frac{I}{\hat{I}}, \quad N^* = \frac{N}{\hat{N}}, \quad E^* = \frac{E}{\hat{E}}, \quad P^* = \frac{P}{\hat{P}}, \quad x^* = \frac{x}{\hat{X}}, \quad t^* = \frac{t}{\tau}. \tag{12}$$

9

By assigning

$$\hat{A} = \hat{I} = \frac{k_7}{k_5}, \;\; \hat{N} = \hat{E} = k_7, \;\; \hat{P} = k_7^2,$$

$$\hat{X} = L, \;\; \tau = \frac{1}{k_6 k_7}. \tag{13}$$

and upon dropping the asterisks from the dimensionless variables, we have a dimensionless system of equations given by

$$\frac{\partial A}{\partial t} = aIE - bA, \tag{14}$$

$$\frac{\partial I}{\partial t} = \frac{\partial}{\partial x}\left(d_I I \frac{\partial I}{\partial x} + d_{cN} I \frac{\partial N}{\partial x} - d_{c\eta} I \frac{\partial A}{\partial x}\right) - aIE + c(N + dA - I), \tag{15}$$

$$\frac{\partial N}{\partial t} = \frac{\partial}{\partial x}\left(d_N N \frac{\partial N}{\partial x} - \overline{\eta} N \frac{\partial A}{\partial x}\right) + N(1 - N), \tag{16}$$

$$\frac{\partial E}{\partial t} = fN(1 - N) - gEP, \tag{17}$$

$$\frac{\partial P}{\partial t} = d_P \frac{\partial^2 P}{\partial x^2} + uNE - vP, \tag{18}$$

where

$$a = \frac{k_1}{k_6}, \;\; b = \frac{k_2}{k_6 k_7}, \;\; c = \frac{k_3 k_5}{k_6 k_7}, \;\; d = \frac{k_4}{k_5}, \;\; f = \frac{k_8}{k_6}, \;\; g = \frac{k_7 k_9}{k_6},$$

$$u = \frac{k_{10}}{k_6 k_7}, \;\; v = \frac{k_{11}}{k_6 k_7}, \;\; d_I = \frac{D_I}{k_5 k_6 L^2}, \;\; d_{cN} = \frac{D_c D_N}{k_6 L^2}, \tag{19}$$

$$d_{c\eta} = \frac{D_c \eta}{k_5 k_6 L^2}, \;\; d_N = \frac{D_N}{k_6 L^2}, \;\; \overline{\eta} = \frac{\eta}{k_5 k_6 L^2}, \;\; d_P = \frac{D_P}{k_6 k_7 L^2}.$$

3.2 *Boundary and Initial Conditions and Parameter Values*

We now specify appropriate boundary and initial conditions for the dimensionless model equations (14)–(18). In reality, the spatial and temporal domains are effectively infinite, though for computational purposes we consider a one dimensional region with $x \in [0, 1]$. In addition, we impose no flux boundary conditions on all five variables of interest. That is, at $x = 0$ and $x = 1$ we have

$$\frac{\partial A}{\partial x} = \frac{\partial E}{\partial x} = \frac{\partial P}{\partial x} = 0,$$

$$d_I I \frac{\partial I}{\partial x} + d_{cN} I \frac{\partial N}{\partial x} - d_{c\eta} I \frac{\partial A}{\partial x} = 0, \tag{20}$$

$$d_N N \frac{\partial N}{\partial x} - \bar{\eta} N \frac{\partial A}{\partial x} = 0.$$

Furthermore, we assume that the initial conditions reflect a cluster of cell matter migrating from left to right as ECM is proteolysed to aid in the haptotactic migration. Initially, no protease is present in the system and cells are not actively adhered to the ECM. This is reflected by the absence of active integrins and an inactive integrin level which is proportional to the cell matter density. Hence we have $A(x,0) = 0$, $I(x,0) = I_0 N(x,0)$, $N(x,0) = e^{-100x^2}$, $E(x,0) = E_0(1-N(x,0))$, $P(x,0) = 0$, where E_0 represents the normal density of the extracellular matrix, and I_0 is the initial number of inactive integrins per unit of cell matter.

To demonstrate the possible behaviours described by this model, the parameter values were estimated using experimental results and values used in other mathematical models whenever possible. Sherratt and Murray (1990) have estimated that random cell motility ranges from $3 \times 10^{-9} \text{cm}^2\text{s}^{-1}$ to $6.9 \times 10^{-11} \text{cm}^2\text{s}^{-1}$. Various length scales are appropriate depending on the particular area of application of the model. Here we will consider a length scale of approximately 3mm. This is the distance considered to facilitate successful angiogenesis for transplanted tumours (Orme and Chaplain, 1996) - one example of cell migration. Owen and Sherratt (1997) and others (Sherratt and Nowak, 1992; Marusic *et al.*, 1994) state that the cell cycle time can be taken as around 100 hours, which we take as our representative timescale. With these key dimensional estimates in mind, we estimate the dimensionless cell matter diffusion coefficient to be in the range 10^{-3} to 10^{-4}.

Where experimental data was lacking, parameter values were chosen to fit known qualitative behaviour of the species in question. Given that protease dynamics occur on a much shorter timescale than cell proliferation and migration (Mignatti and Rifkin, 1993), the coefficients of proteolysis and protease decay were taken to be relatively large. Following similar models of chemotactic and haptotactic cell migration due to Perumpanani *et al.* (1998, 1999), here we consider a protease coefficient of order 10^{-2} or less. Furthermore, in a manner similar Anderson *et al.* (2000) we take the coefficient of haptotactic migration to be similar to, or an order of magnitude greater than, that of random cell motion. This relationship stems from experimental results due to Terranova *et al.* (1985), Stokes and Lauffenburger (1991) and Bray (1992).

With regard to the rate constants for integrin production, binding and unbinding, we take a similar approach to Sherratt *et al.* (1993). That is, the kinetic terms for integrins are quite fast compared with the timescale of cell

migration. The "diffusion" coefficient for inactive integrins, d_I, was taken to be quite large when compared with the random cell motility coefficient, d_N. This reflects the protrusion of lamellipodia, carrying with them large numbers of inactive integrins while only minute amounts of cell matter are disturbed.

3.3 Simulations

Examples of model solutions are now presented including consideration of parameter value variations. All solutions have been calculated using Numerical Algorithms Group fortran routine D03PCF.
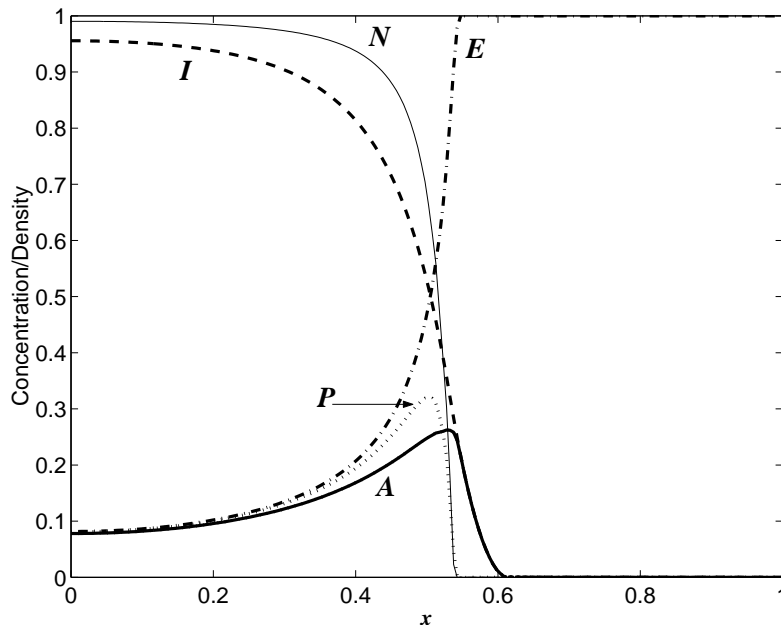

Fig. 1. Plot of all five species for dimensionless time $t = 15$ using equations (14)–(18). Parameter values used here and in Figure 2 are $\bar{\eta} = 0.01$, $d_N = 0.001$, $d_P = 0.005$, $d_I = 10$, $d_{cN} = 0.001$, $d_{c\eta} = 0.01$, $a = b = u = v = 1000$, $c = 2000$, $d = 0.1$, $f = 20$, $g = 30$, $E_0 = 1$, $I_0 = 1$.

Figure 1 shows an example of the state of the system at a particular dimensionless time value, $t = 15$, with the indicated parameter values. Over time the front of cell matter has steepened, although not to a sharp front for this particular parameter set. The effect of the protrusion term in the inactive integrin equation is clearly visible, with the integrin populations edging in front of the cell matter front. The protruded inactive integrins are quickly activated through adhesion to ligands in the ECM. This has the effect of creating an appropriate gradient in $A(x, t)$ to allow haptotactic cell migration from left to right.

In Figure 2(a) we present what appears to be travelling wave behaviour in the
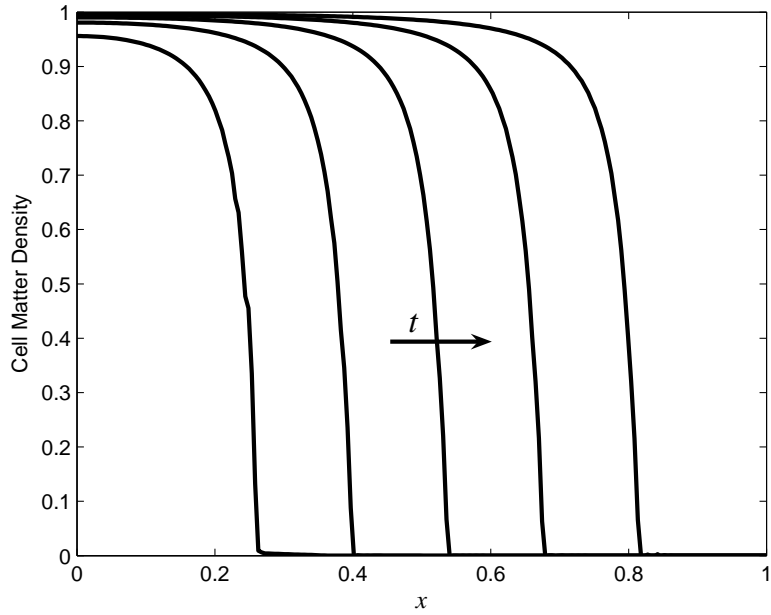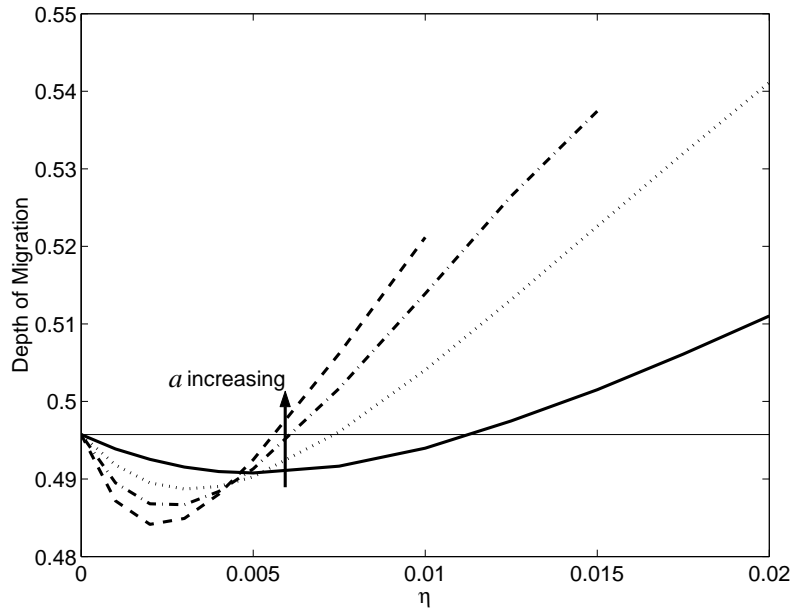
Fig. 2. (a) Plot of cell matter profiles for dimensionless times $t = 5, 10, 15, 20, 25$, using equations (14)–(18), with parameter values as in Figure 1. Solutions are calculated using $\Delta t = 0.01$ for $t = [0, 25]$, and 210 spatial nodes. (b) Cell migration depth vs haptotactic coefficient for various values of the integrin activation coefficient a ($a = 0, 250, 500, 750, 1000$), at dimensionless time $t = 15$.

cell matter density. After an initial setup time, cells migrate from left to right with an approximately constant wavespeed and shape, leaving behind them the maximum scaled cell density of $N(x, t) = 1$. This hypothesis regarding travelling wave solutions will be investigated further in Section 5.

13

Figure 2(b) shows the effect on migration depth of different haptotactic coefficients, for various integrin activation coefficients. Here the depth of migration is defined to be the point in space at which $N(x,t) = 0.5$. It is observed that for all curves with $a > 0$, the use of small haptotactic coefficients results in a decrease in migration depth compared with the case of solely diffusion–driven cell movement, which has a migration depth identical to that of the $a = 0$ case. This is due to the fact that for small $\bar{\eta}$, nonlinear diffusion is the dominant migration process. The cell front diffuses to a location ahead of the maximum level of active integrins, and as such, small increases in the haptotactic coefficient cause increases in backwards (from right to left) cell migration. As $\bar{\eta}$ is increased, the migration depth reaches a minimum value for each a curve, before increasing in an approximately linear manner. With these higher $\bar{\eta}$ values, the backwards migration due to haptotaxis has caused sufficient sharpening of the cell front to place it to the left of the maximum density of active integrins and thus, any increase in the value of $\bar{\eta}$ results in an increase in the haptotactic migration from left to right.

The increase in haptotactic migration continues until it is no longer possible to compute solutions with the computational techniques used for this work. Given that the numerical solution method used here is the Numerical Algorithms Group (NAG) routine D03PCF, a parabolic PDE solver, increases in the haptotactic coefficient that cause the system to become dominantly hyperbolic (the haptotaxis term far outweighs the diffusion term in the cell and integrin equations) lead to the model equations being incompatible with the NAG routine.

Variations to other system parameters were also considered. The successful migration of cells is quite sensitive to the protease diffusion coefficient, d_P. For small values of the parameter, the protease distribution is localised at the cell migration front and thus aids in the construction of an adhesion gradient upon which cells may migrate. For larger values of d_P, the adhesion gradient is lower and the cells undergo far less migration.

Similarly, for values of the dimensionless proteolysis coefficient, g, that are large in comparison with the dimensionless protease production coefficient f, decreased migration is displayed. While modest increases in g can lead to increased migration of cells, when the parameter is too high in relation to f the ECM is degraded too quickly, and the resulting gradient in active integrins is too small to aid migration to any great extent. A comparable result is found when investigating the protease production and decay coefficients, which must also be kept closely balanced.

It is also important to consider the ratio of the dimensionless integrin binding and unbinding coefficients, a and b. Continual binding and unbinding of integrins is necessary for cells to migrate successfully. This is indicated in the

numerical solutions of the model developed in this chapter by increasing a and decreasing b. Such parameter changes away from those used in the successful migration shown in Figure 2(a), result in decreased migration. With a low value for the dimensionless unbinding coefficient the positive gradient in active integrins, behind the front of cells, is not able to form and the excessive adhesion of cells to the ECM causes a decrease rather than an increase in migration.

4 Implications of Fast Integrin Kinetics Assumptions

In this section we consider the possibility of simplifying the five equation model of Section 2, through the assumption of fast integrin kinetics. These simplifications allow the development of a relationship between this novel integrin–mediated haptotaxis model and previous ECM–mediated models.

4.1 Fast Integrin Kinetics and a Simplified Model

Returning to the dimensionless system of equations (14)–(18), we now consider a model simplification based on the assumption of fast integrin kinetics. Integrin binding and production occur on a much shorter timescale than processes such as cellular proliferation and migration. With this in mind, consider equations (14) and (15), and let $a = \dfrac{\alpha}{\varepsilon}$, $b = \dfrac{\beta}{\varepsilon}$, $c = \dfrac{\gamma}{\varepsilon}$, where we take α, β and $\gamma \sim \mathcal{O}(1)$ and $\varepsilon \ll 1$. By multiplying equations (14) and (15) by ε, then rearranging the resulting equations and considering only the terms of $\mathcal{O}(\varepsilon^0)$, we have

$$\alpha IE - \beta A = 0, \tag{21}$$
$$-\alpha IE + \gamma(N + dA - I) = 0. \tag{22}$$

Rearranging the first of these equations gives

$$A = \frac{a}{b}IE. \tag{23}$$

Substituting the above expression for A into the second of the $\mathcal{O}(\varepsilon^0)$ equations and rearranging, gives

$$I = \frac{N}{1 + \dfrac{aE}{c}\left(1 - \dfrac{cd}{b}\right)}. \tag{24}$$

15

Now consider the case where activation of integrins occurs slower than integrin production, that is $\frac{a}{c} < 1$, integrin binding and unbinding occur at similar rates, that is $\frac{a}{b} \sim \mathcal{O}(1)$, and $0 < d < 1$ sufficiently small that $\frac{ad}{b} < 1$. Parameter relationships such as these give rise to the numerical results shown in Figures 1 and 2, and also produce the inequality

$$\frac{aE}{c}\left(1 - \frac{cd}{b}\right) < 1. \tag{25}$$

Hence, given the above inequality, we may consider the first order approximation of I to be, in dimensionless form

$$I = N. \tag{26}$$

Substituting equations (23) and (26) into the third, fourth and fifth of equations (11), using the scalings given in equations (13) and dimensionless parameters in equations (19), gives the following three equation model, valid in the case of fast integrin kinetics:

$$\begin{aligned}
\frac{\partial N}{\partial t} &= \nabla \cdot \left(D_N^S(\cdot)N\nabla N - \eta^S(\cdot)N\nabla(NE)\right) + N(1-N), \\
\frac{\partial E}{\partial t} &= fN(1-N) - gPE, \\
\frac{\partial P}{\partial t} &= d_P\nabla^2 P + uNE - vP.
\end{aligned} \tag{27}$$

where $D_N^S(\cdot) = \frac{D_N(\cdot)}{k_6 L^2}$ and $\eta^S(\cdot) = \frac{\eta(\cdot)k_1}{k_2 k_6 L^2}$ are the scaled, undetermined cell matter diffusion and haptotaxis coefficients.

To investigate this simplified model numerically, we again set $\eta(\cdot)$ and $D_N(\cdot)$ to be constants, η and D_N, and restrict our attention to one spatial dimension, with $x \in [0,1]$. Again, this leads to the dimensionless cell matter diffusion coefficient $d_N = \frac{D_N}{k_6 L^2}$, the dimensionless haptotactic coefficient $\overline{\eta}_3 = \frac{\eta k_1}{k_2 k_6 L^2}$, and all other parameters are as stated in Section 3.1.

(a)

(b)

17

(c)

(d)
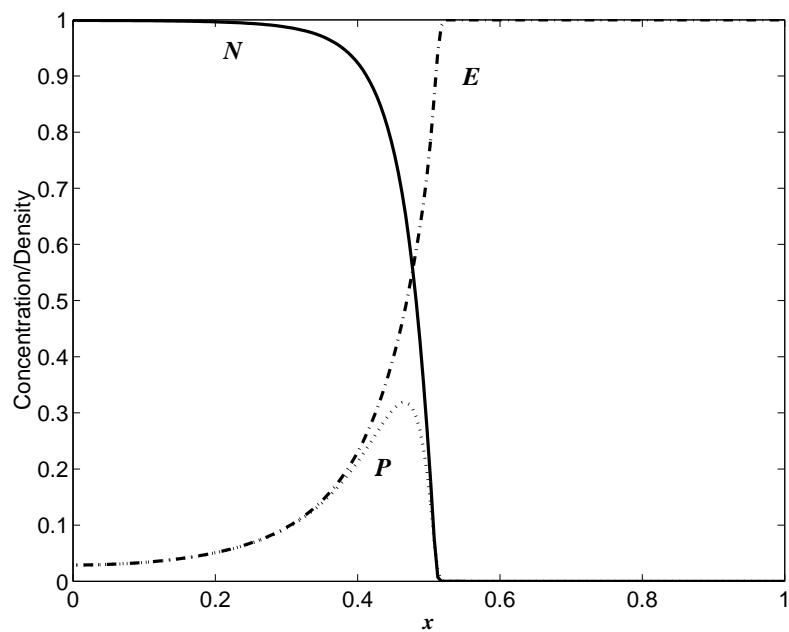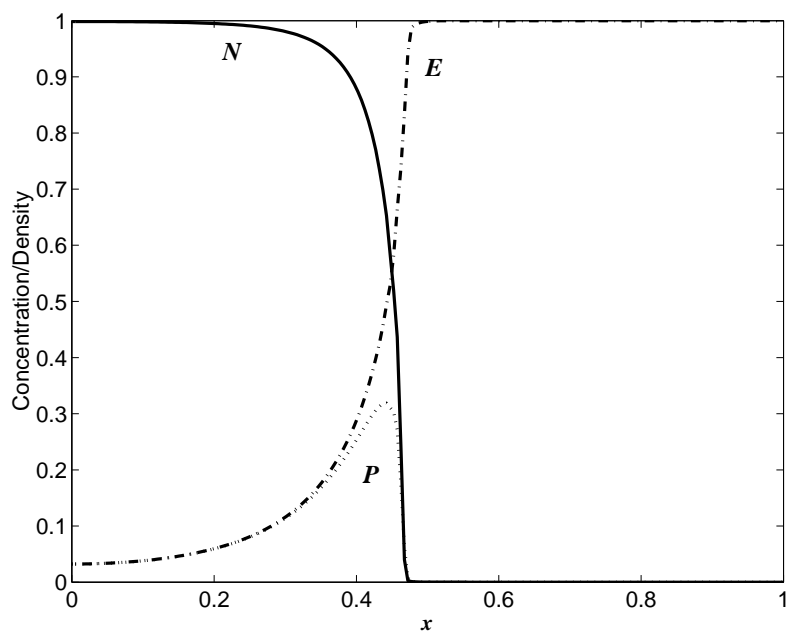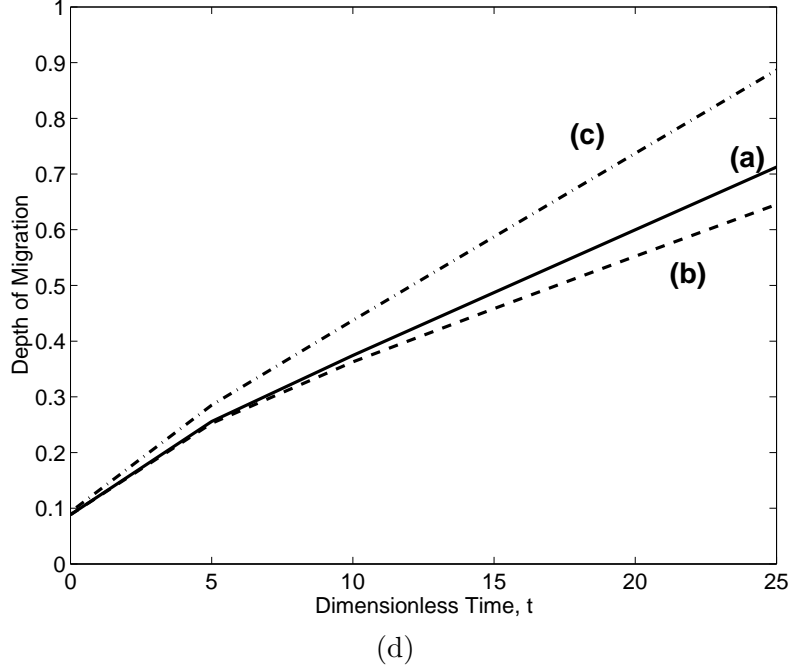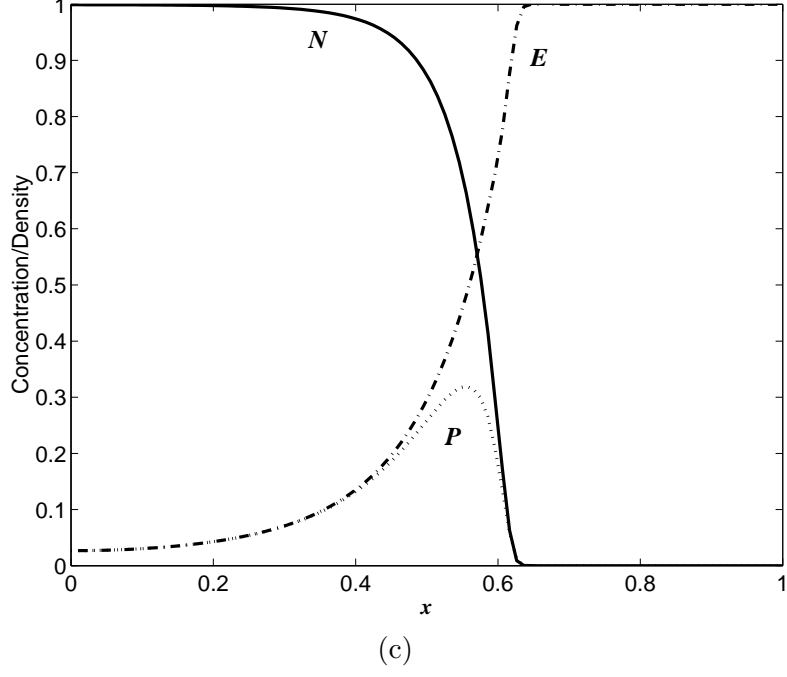
Fig. 3. Plots (a), (b) and (c) show cell matter $N(x,t)$, ECM $E(x,t)$ and protease $P(x,t)$ at the dimensionless time value $t = 15$. Plot (a) is produced using the full model, equations (14)–(18), with parameter values of $\overline{\eta} = 0.001$, $d_N = 0.001$, $d_P = 0.005$, $d_I = 10$, $d_{cN} = 0.001$, $d_{c\eta} = 0.01$, $a = b = u = v = 1000$, $c = 2000$, $d = 0.1$, $f = 20$, $g = 30$. Plot (b) uses equations (27), the reduced three equation model, with the equivalent parameter values of $\overline{\eta}_3 = 0.001$, $d_N = 0.001$, $d_P = 0.005$, $u = v = 1000$, $f = 20$, $g = 30$. Plot (c) is produced using similar equations and parameter values to plot (b), though an altered cell flux, proportional to $N\frac{\partial E}{\partial x}$, is employed. Plot (d) shows the depth of migration vs time for the three models. Full model (a), reduced model (b), ECM–mediated model (c).

18

Numerical simulations show that the simplified model is a good approximation to the full, integrin–mediated haptotaxis model, provided we are considering a case where integrin kinetics are indeed fast. Shown in Figure 3 is a numerical comparison between the full, five equation model, the simplified version and a traditional ECM–mediated model (identical to equations (27) with the exception of the cell flux, which is given by $\eta N \dfrac{\partial E}{\partial x}$), with parameter values which indicate fast integrin kinetics. We note that the simplified model produces a cell matter profile (and protease profile) which is slightly steeper at the front, than the profile displayed in the full model simulation. This is due to the introduction of a "backwards diffusion" term as a result of the simplification $A = \dfrac{a}{b} NE$. Both the full model and the simplified model produce reduced cell migration depths when compared with the traditional ECM–mediated model.

Figure 3 (d) provides a comparison of the depth reached over time, by populations of migrating cells described by each of the three models in (a)–(c). We note that, compared with the full integrin–mediated model, the simplified $\nabla(NE)$ haptotaxis model has a slightly lower speed of migration due to the introduction of a backwards diffusion term in the cell matter flux. On the other hand, the ECM–mediated haptotaxis model has a much higher speed of migration as it is similar to the simplifed model without the backwards diffusion term. The result shown suggests that previous ECM–mediated haptotaxis models overestimate the speed of haptotactic cell migration when compared with the integrin–mediated model which takes into account cell adhesion processes.

4.2 A Relationship Between Integrin–mediated and ECM–mediated Haptotaxis Models

In this section, we use the pseudo–steady state assumptions described above, along with specific choices for the cell diffusion and haptotaxis coefficients to show that the ECM–mediated haptotaxis models of other researchers in this area can be derived using simplifications of the novel, integrin–mediated haptotaxis model developed in this paper.

Consider the cell matter flux from the simplified system of equations (27), given by

$$
\begin{aligned}
\mathbf{J}_N &= -D_N^S(\cdot)N\nabla N + \eta^S(\cdot)N\nabla(NE) \\
&= -D_N^S(\cdot)N\nabla N + \eta^S(\cdot)NE\nabla N + \eta^S(\cdot)N^2\nabla E.
\end{aligned}
\tag{28}
$$

We will show that through using equations (23) and (26), along with specific choices for $D_N^S(\cdot)$ and $\eta^S(\cdot)$, we are able to reduce the migration terms for

19

the cell matter equation of the new integrin–mediated model to those of a general ECM–mediated haptotaxis model. For later reference, we introduce the migration terms for cells in a general ECM–mediated haptotaxis model (including both diffusive and haptotactic components):

$$\mathbf{J}_G = -d(\cdot)\nabla N + h(\cdot)N\nabla E, \tag{29}$$

where $d(\cdot)$ is the unspecified, non–constant cell diffusion coefficient and $h(\cdot)$ is the unspecified, non–constant haptotactic coefficient.

We note that to match coefficients of ∇E in the above expression and equation (28), we require

$$\eta^S(\cdot) = \frac{h(\cdot)}{N}. \tag{30}$$

Substitution of this expression for $\eta^S(\cdot)$ into equation (28), and then matching the coefficients of ∇N requires the scaled diffusion coefficient of the integrin–mediated model to be

$$D_N^S(\cdot) = \frac{d(\cdot) + h(\cdot)E}{N}. \tag{31}$$

That is, through careful definition of the haptotactic and diffusion coefficients using equations (30) and (31), coupled with the assumption of fast integrin kinetics, ECM–mediated haptotaxis models can be thought of as simplifications of the integrin–mediated haptotaxis model presented here.

For example, the ECM–mediated haptotaxis model of Perumpanani *et al.* (1999) has in its cell equation, migration terms of the form

$$\mathbf{J}_p = kN\nabla E,$$

where k is the constant coefficient of haptotactic migration, and the model does not include cell diffusion (that is, $d(\cdot) = 0$). This form for the migration terms can be arrived at from that of the full integrin–mediated haptotaxis model through the assumption of fast integrin kinetics, the definition of the scaled haptotactic coefficient as $\eta^S(\cdot) = \dfrac{k}{N}$ and the diffusion coefficient as $D_N^S(\cdot) = \dfrac{kE}{N}$. Furthermore, if we were to set $k_8 = 0$ and $D_P = 0$ in the fast integrin kinetics model, that entire model can be simplified to the model described by Perumpanani *et al.* (1999).

5 Further Simplification and Travelling Wave Analysis

It was noted earlier that the cell matter profiles displayed in Figure 2 appear to be moving as a travelling wave of constant speed and shape. Here we consider further simplifications to the integrin–mediated haptotaxis model which has been reduced to the three equation, fast integrin kinetics model described in dimensionless equations (27). Further simplifications allow an analytical investigation of the existence of travelling waves of migrating cells, described by the model. Once more we consider a single spatial dimension, x, and take $\eta(\cdot)$ and $D_N(\cdot)$ to be constants. The model to be investigated is then

$$\frac{\partial N}{\partial t} = \frac{\partial}{\partial x}\left(d_N N \frac{\partial N}{\partial x} - \bar{\eta}_3 N \frac{\partial(NE)}{\partial x}\right) + N(1-N), \tag{32}$$

$$\frac{\partial E}{\partial t} = fN(1-N) - gEP, \tag{33}$$

$$\frac{\partial P}{\partial t} = d_P \frac{\partial^2 P}{\partial x^2} + uNE - vP. \tag{34}$$

To simplify the above model we consider a situation where protease production and decay, as well as ECM production and proteolysis occur on a shorter timescale than that of cellular proliferation and migration. Furthermore, with only small–scale protease diffusion, we consider the following pseudo–steady state equations resulting from equations (33) and (34).

$$fN(1-N) - gEP = 0, \tag{35}$$
$$uNE - vP = 0. \tag{36}$$

Equation (36) implies that $P = \dfrac{u}{v}NE$ which can then be substituted into the equation (35) to allow for an approximation of E in terms of N alone. Upon substitution and rearrangement, we have

$$E = \sqrt{\frac{fv}{gu}(1-N)}. \tag{37}$$

This approximation may then be substituted into equation (32) to give the following partial differential equation for N.

$$\frac{\partial N}{\partial t} = \frac{\partial}{\partial x}\left(d_N N \frac{\partial N}{\partial x} - \bar{\eta}_1 N \frac{\partial(N\sqrt{1-N})}{\partial x}\right) + N(1-N), \tag{38}$$

where $\overline{\eta}_1 = \sqrt{\dfrac{fv}{gu}}$, $\overline{\eta}_3 = \sqrt{\dfrac{k_8 k_{11}}{k_7 k_9 k_{10}}} \left(\dfrac{\eta k_1}{k_2 k_6 L^2} \right)$.

To continue with the travelling wave analysis, we consider the amount of cell diffusion to be negligible when compared with cell proliferation and hapto-tactic migration, and hence we take $d_N \approx 0$. We now introduce the travelling wave variable $z = x - wt$, where w is the positive wavespeed. Upon changing variables, equation (38) becomes a second order ordinary differential equation (ODE) given by

$$
\begin{aligned}
-w N_z = {} & -\overline{\eta}_1 (N_z)^2 \sqrt{1-N} + \frac{3\overline{\eta}_1 N (N_z)^2}{2\sqrt{1-N}} - \overline{\eta}_1 N N_{zz} \sqrt{1-N} \\
& + \frac{\overline{\eta}_1 N^2 (N_z)^2}{4(1-N)^{3/2}} + \frac{\overline{\eta}_1 N^2 N_{zz}}{2\sqrt{1-N}} + N(1-N),
\end{aligned} \tag{39}
$$

where subscript z denotes differentiation with respect to the travelling wave variable.

This ODE may be rewritten as a system of two, first order ODEs using the substitution $U(z) = \dfrac{dN}{dz}$. These two, first order ODEs may then be used to conduct a phase plane analysis of the system. Upon substitution we have the equations

$$
\begin{aligned}
N_z = {} & U, \\
U_z \left[\overline{\eta}_1 N \sqrt{1-N} - \frac{\overline{\eta}_1 N^2}{2\sqrt{1-N}} \right] = {} & wU + N(1-N) - \overline{\eta}_1 U^2 \sqrt{1-N} \\
& + \frac{3\overline{\eta}_1 N U^2}{2\sqrt{1-N}} + \frac{\overline{\eta}_1 N^2 U^2}{4(1-N)^{3/2}}.
\end{aligned} \tag{40}
$$

The steady states of the first order system are then found by solving for the points of intersection of the N and U nullclines, and are given by

$$
\text{SS}_1 : \left(\overline{N}_1, \overline{U}_1 \right) = (0,0); \qquad \text{SS}_2 : \left(\overline{N}_2, \overline{U}_2 \right) = (1,0), \tag{41}
$$

which are indicative of the normal tissue situation where the cell level is zero (SS_1), and the fully migrated state where the cell level is at its scaled maximum (SS_2). Returning to the existence of travelling wave solutions to this system, we hence require the possibility of a connection between SS_2 and SS_1 in the (N, U) phase plane.

Considering the second of equations (40), we note that the U_z equation be-

comes singular when

$$\bar{\eta}_1 N \sqrt{1 - N} - \frac{\bar{\eta}_1 N^2}{2\sqrt{1 - N}} = 0. \tag{42}$$

Solving this equation for N we find that singularities occur along the lines $N = 0$ and $N = \frac{2}{3}$, and note that the equation is undefined for $N = 1$. As in Pettet (1996); Marchant (1999); Perumpanani *et al.* (1999) and Pettet *et al.* (2001) we will refer to these lines as *walls of singularities* – lines which cannot be crossed by solution trajectories in the phase plane except at points where the walls coincide with the U nullcline. These coincidental points were also discussed in Pettet (1996); Marchant (1999); Perumpanani *et al.* (1999) and Pettet *et al.* (2001) and are known as *holes in the walls*.

Solving the U nullcline equations with conditions imposed by the walls of singularities, we find the following holes in the walls. Along the $N = 0$ wall, solution curves may pass through the points

$$(N_{H1}, U_{H1}) = (0, 0),$$
$$(N_{H2}, U_{H2}) = \left(0, \frac{w}{\bar{\eta}_1}\right). \tag{43}$$

While for the $N = \frac{2}{3}$ wall, solution curves may pass through the points

$$(N_{H3}, U_{H3}) = \left(\frac{2}{3}, \frac{1}{2\sqrt{3}\bar{\eta}_1}\left(-w + \sqrt{w^2 - \frac{8\bar{\eta}_1}{3\sqrt{3}}}\right)\right),$$
$$(N_{H4}, U_{H4}) = \left(\frac{2}{3}, \frac{1}{2\sqrt{3}\bar{\eta}_1}\left(-w - \sqrt{w^2 - \frac{8\bar{\eta}_1}{3\sqrt{3}}}\right)\right). \tag{44}$$

Initially, the walls of singularities at $N = 0$ and $N = \frac{2}{3}$ indicated that it would not be possible for a solution trajectory to join the two steady states, and as such no travelling wave solutions could exist for this model. However, the existence of holes in the walls at the trivial steady state and at two points on the $N = \frac{2}{3}$ wall may allow for a connection between the two steady states. Note that through investigation of the phase plane in Figure 4, it is evident that the hole given by (N_{H3}, U_{H3}) is the one that leads to connection between the steady states, and as such, for any given haptotactic coefficient we require

23

wavespeeds above the minimum value of

$$w_{min} = \sqrt{\frac{8\overline{\eta}_1}{3\sqrt{3}}}. \tag{45}$$

For wavespeeds below this value, the coordinates of the hole in the wall are complex–valued and hence, a connection between the steady states does not exist.

Substituting the parameters used in Figures 1 and 2 into the above equation produces a minimum wavespeed of $w_{min} = 0.112$. The wavespeed of cells shown in Figures 1 and 2 is $w \approx 0.25$, which is well above the suggested minimum and supports the consistency of the results regarding the minimum wavespeed.

Here we have arrived at a key finding of this research, namely that there is a minimum wavespeed for travelling wave solutions of this model. In particular, it has been shown that

$$w_{min}^2 \propto \sqrt{\overline{\eta}_1}. \tag{46}$$

Furthermore, Figure 2(b) shows that the wavespeed (or depth of migration) is closely related to the dimensionless rate of integrin binding, a. Given that the dimensioned form of $\overline{\eta}_1$ is proportional to $\dfrac{k_1}{k_2}$, this dependence of the wavespeed on integrin binding includes the ratio of integrin binding to unbinding $\dfrac{k_1}{k_2}$. That is, the wavespeed of haptotactically migrating cells is closely linked to the rate at which cells bind to ECM compared with the rate at which they release from the matrix.

In Figure 4, the solution directions and nullclines indicate that a trajectory may leave the $(1,0)$ steady state, following the U nullcline to pass through the third hole in the wall (N_{H3}, U_{H3}) before again closely following the U nullcline to enter the steady state at $(0,0)$. The existence of the connection between $(0,0)$ and $(1,0)$ in the (N,U) phase plane supports the hypothesis derived from the numerical simulations of the model given in equations (14)–(18), that the system does support travelling wave solutions.

Figure 5 shows a numerical solution of equation (39). Due to the nonlinearity of equation (39) and its singularity at $N = \frac{2}{3}$, it was not possible to solve the equation for all z. Instead, the solution was calculated in two parts: from $-\infty$ forward toward zero, and from ∞ back toward zero. The solution shown is a wave of similar shape to those in Figure 2(a). Note however that the front of the wave is not sharp as it was in Figure 2(a) due to the earlier assumption that $d_N \approx 0$. Keeping in mind the lack of front-sharpness, the
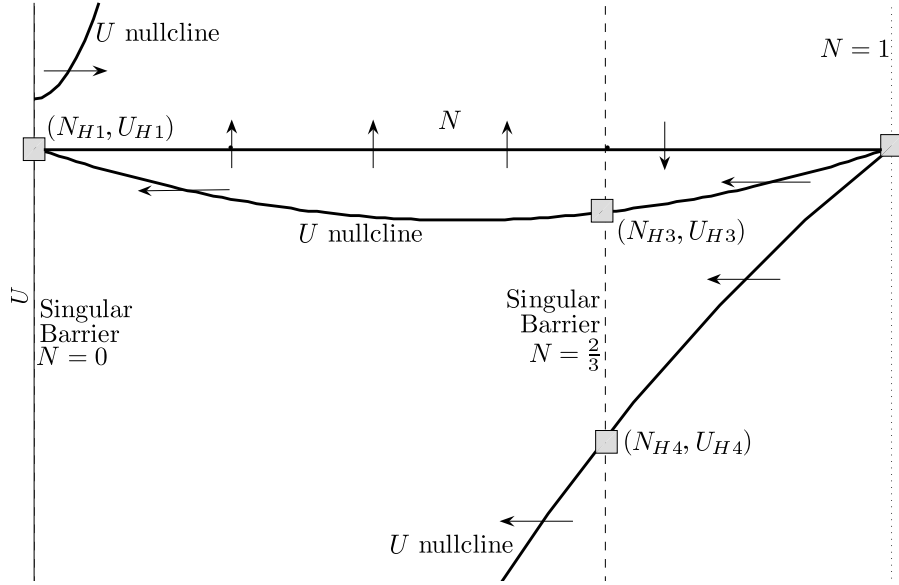
Fig. 4. Schematic view of the (N, U) phase portrait for equations (40) demonstrating the possibility of a connection between the steady states (diagram not drawn to scale). The U nullclines and singular barriers are indicated and the N nullcline is the dotted horizontal axis. The holes in the wall are shown as grey squares.
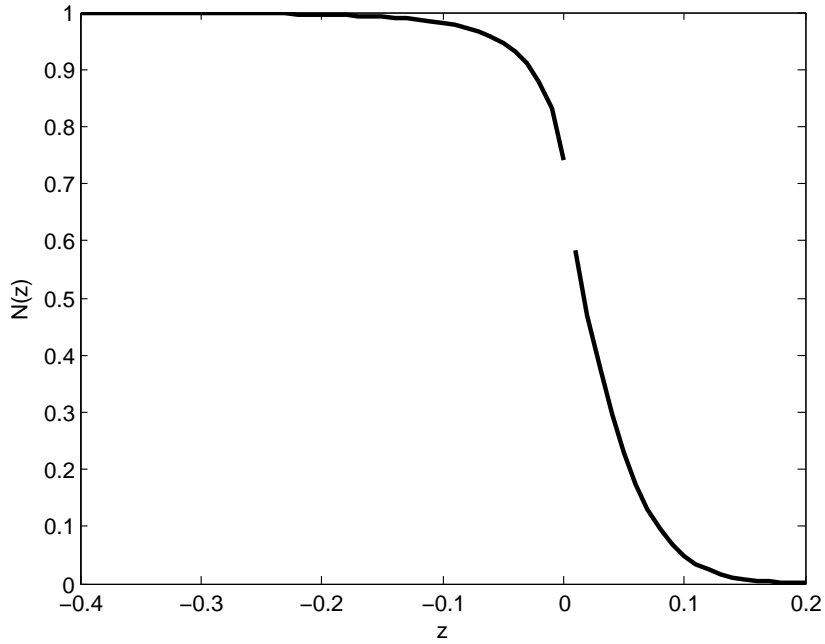

Fig. 5. Plot of $N(z)$ vs z from a solution of the travelling wave equations (39), with $\bar{\eta}_1 = 0.01$ and $w = 0.25$. Note the singularity at $N = \frac{2}{3}$ where the solution was not able to be computed.

extent of the similarity between the solution shown in Figure 5 and those in Figure 1 is further substantiation of the existence of travelling wave solutions and the findings above regarding the wavespeed of cells undergoing haptotactic migration.

25

6 Conclusion

Haptotaxis is an important method of cell migration in wound healing, tumour invasion and innovative tissue engineering strategies. Here we have presented a mathematical model which provides a description of haptotactic cell migration. The description of the model as a novel one, arises from the inclusion of mathematical descriptions of important processes such as integrin mediated cell–ECM adhesion, the functional activation of integrins by the ECM, recruitment of inactive integrins to sites of adhesion and the protrusion by cells of integrin–rich lamellipodia.

Numerical solutions show successful haptotactic migration over the extracellular matrix and suggest travelling wave solutions exist for the model equations. Such travelling waves are substantiated through a phase plane analysis of a simplified model. The numerical solutions show a biphasic relationship between the depth of cell migration and the magnitude of the haptotactic response, where for small haptotactic coefficients the migration of cells is actually slowed.

Under the assumption of fast integrin kinetics, we have developed a reduced three equation model of haptotactic cell migration which provides a good approximation to the full model. This reduced model differs from the novel integrin–mediated model and the standard ECM–mediated models in that the cells migrate in response to a gradient in the product of cell and ECM densities. An analytical relationship between this simplified model and ECM–mediated models was then developed, demonstrating that the standard models can be thought of as a subset of the integrin–mediated model with fast receptor kinetics, along with appropriate choices for the diffusion and haptotactic coefficients.

Finally, a travelling wave analysis was undertaken for a further simplified version of the cell migration model. The phase portrait constructed for this simplified model exhibits a connection between steady states in the phase plane and this confirms the possibility of wavelike solutions to the model as suggested by the numerical simulations. The phase plane for this model exhibits a number of walls of singularities and gates through which solution trajectories may pass – one of which allows for trajectories to join the two steady states of the system. The requirement for a real–valued hole in the wall also provides a condition on the minimum allowable wavespeed for a travelling wave solution. It is shown that the minimum wavespeed clearly depends on the ratio of integrin binding to integrin unbinding, $\dfrac{k_1}{k_2}$. This is a key finding of this work in that the dependence of haptotactic migration on cell to ECM adhesion is demonstrated through the relationship between the haptotactic

wavespeed and the integrin binding coefficients.

With the inclusion of integrins in mathematical models of haptotaxis, in the manner that has been shown here, it becomes possible to model adhesion related processes such as cell death due to anoikis and cancer treatment strategies such as integrin blocking and to consider their effects upon the invasion of haptotactically migrating cells. While this new model does give a more complete description of the biological processes involved in haptotactic cell migration, the lack of available data (for example, regarding parameter values) suggests that further experimental work in this area is required to validate this new description of haptotaxis.

References

A.R.A. Anderson and M.A.J. Chaplain, (1998). Continuous and discrete mathematical models of tumor induced angiogenesis. *Bull. math. Biol.* 60, 877–900.

A.R.A. Anderson, M.A.J. Chaplain, E.L. Newman, R.J.C. Steele, and A.M. Thompson, (2000). Mathematical modelling of tumour invasion and metastasis. *Journal of Theoretical Medicine.* 2, 129–154.

A.E. Aplin, A. Howe, S.K. Alahari and R.L. Juliano, (1998). Signal transduction and signal modulation by cell adhesion receptors: The role of integrins, cadherins, immunoglobulin–cell adhesion molecules, and selectins. *Pharmacological Reviews.* 50, 197–252.

D. Bray (1992). *Cell Movements.* Garland Publishing, New York.

S.B. Carter, (1965). Principles of cell motility: The direction of cell movement and cancer invasion. *Nature.* 208, 1183–1187.

John C. Dallon and Hans G. Othmer, (1997). A discrete cell model with adaptive signalling for aggregation of *Dictyostelium discoideum. Phil. Trans. R. Soc. Lond. B.* 352(1351), 391–417.

John C. Dallon and Hans G. Othmer, (1998). A Continuum Analysis of the Chemotactic Signal Seen by *Dictyostelium discoideum. J. theor. Biol.* 194, 461–483.

P.A. DiMilla, K.Barbee and D.A. Lauffenburger, (1991). Mathematical model for the effects of adhesion and mechanics on cell migration speed. *Biophys. J.* 60, 15–37.

S.M. Frisch and E. Ruoslahti, (1997). Integrins and anoikis. *Current Opinion in Cell Biology.* 9, 701–706.

T. Hoefer, J.A. Sherratt and P.K. Maini, (1995). Dictyostelium discoideum: cellular self–organization in an excitable biological medium. *Proc. R. Soc. Lond. B.* 259, 249–257.

T. Hoefer, J.A. Sherratt and P.K. Maini, (1995). Cellular pattern formation during Dictyostelium aggregation. *Physica D.* 85, 425–444.

D. Lauffenburger, (1989). A simple model for the effects of receptor–mediated cell–substratum adhesion on cell migration. *Chemical Engineering Science.* 44(9), 1903–1914.

D.A. Lauffenburger and J.J. Linderman, (1993). *Receptors: Models for Binding, Trafficking and Signalling.* Oxford University Press.

B.D. MacArthur, (2002). Mathematical modelling of malignant growth and invasion. *PhD Thesis*, University of Southampton.

P.K. Maini, (1989). Spatial and spatio–temporal patterns in a cell–haptotaxis model. *J. Math. Biol.* 27, 507–522.

G. Maheshwari and D.A. Lauffenburger, (1998). Deconstructing (and reconstructing) cell migration. *Microscopy Research and Technique.* 43, 358–368.

B.Marchant, (1999). Modelling Cell Invasion. *DPhil Thesis*, University of Oxford.

M. Marusic, Z. Bajzer, J.P. Freyer and S. Vuk-Pavlovic, (1994). Analysis of growth of multicellular tumor spheroids by mathematical models. *Cell Prolif.* 27, 73–94.

P. Mignatti and D.B. Rifkin, (1993). Biology and biochemistry of proteinases in tumor invasion. *Physiol. Rev.* 73, 161–195.

J.D. Murray, (1993). *Mathematical Biology.* 2nd Edition. New York: Springer–Verlag.

L. Olsen, J.A. Sherratt and P.K. Maini, (1995). A mechanical model for adult dermal wound contraction and the permanence of the contracted tissue displacement profile. *J. theor. Biol.* 177, 113–128.

L. Olsen, J.A. Sherratt and P.K. Maini, (1996). A mathematical model for fibroproliferative wound healing disorders. *Bull. math. Biol.* 58(4), 787–808.

M.E. Orme and M.A.J. Chaplain, (1996). A mathematical model of vascular tumour growth and invasion. *Mathl. Comput. Modelling.* 23(10), 43–60.

H.G. Othmer, B. Lilly and J.C. Dallon, (2000). Pattern formation in a cellular slime mould, in *Numerical Methods for Bifurcation Problems and Large Scale Dynamical Systems.* IMA Procedings 119, E. Doedel and L.S. Tuckerman (Eds), pp. 359–383.

M.R. Owen and J.A. Sherratt, (1997). Pattern Formation and Spatiotemporal Irregularity in a Model for Macrophage-Tumour Interactions. *J. theor. Biol.* 189, 63–80.

A.J. Perumpanani, D.L. Simmons, A.J.H. Gearing, *et al.*, (1998). Extracellular matrix-mediated chemotaxis can impede cell migration. *Proc. R. Soc. Lond. B.* 265, 2347–2352.

A.J. Perumpanani and H.M. Byrne, (1999). Extracellular matrix concentra-

tion exerts selection pressure on invasive cells. *European Journal of Cancer.* 35(8), 1274–1280.

A.J. Perumpanani, J. Norbury, J.A. Sherratt and H.M. Byrne, (1996). Biological inferences from a mathematical model for malignant invasion. *Invasion and Metastasis.* 16, 209–221.

A.J. Perumpanani, J.A. Sherratt, J. Norbury and H.M. Byrne, (1999). A two parameter family of travelling waves with a singular barrier arising from the modelling of extracellular matrix mediated cellular invasion. *Physica D.* 126, 145–159.

G.J. Pettet, (1996). Modelling Wound Healing Angiogenesis and Other Chemotactically Driven Growth Processes. *PhD Thesis*, University of Newcastle.

G.J. Pettet, D.L.S. McElwain and J. Norbury, (2001). Lotka-Volterra equations with chemotaxis: walls, barriers and travelling waves *IMA Journal of Mathematics Applied in Medicine and Biology.* 17(4), 395–413.

J.A. Sherratt and J.D. Murray, (1990). Models of epidermal wound healing. *Proc. R. Soc. Lond.* B. 241, 29–36.

J.A. Sherratt and M.A. Nowak, (1992). Oncogenes, anti-oncogenes and the immune response to cancer: a mathematical model. *Proc. R. Soc. Lond.* B. 248, 261–271.

J.A. Sherratt, E. Helene Sage and J.D. Murray, (1993). Chemical control of eukaryotic cell movement: A new model. *J. theor. Biol.* 162, 23–40.

J.A. Sherratt, (1994). Chemotaxis and chemokinesis in eukaryotic cells: The Keller–Segel equations as an approximation to a detailed model. *Bull. math. Biol.* 56(1), 129–146.

W.G. Stetler-Stevenson, S. Aznavoorian and L.A. Liotta, (1993). Tumor cell interactions with the extracellular matrix during invasion and metastasis. *Annu. Rev. Cell Biol.* 9, 541–573.

C.L. Stokes and D.A. Lauffenburger, (1991). Analysis of the roles of microvessel endothelial cell random motility and chemotaxis in angiogenesis. *J. theor. Biol.* 152, 377–403.

V.P. Terranova, R. Diflorio, R.M. Lyall, S. Hic, R. Friesel and T. Maciag, (1985). Human endothelial cells maintained in the absence of fibroblast growth factor undergo structural and functional alterations that are incompatible with their *in vivo* differentiated properties. *J. Cell Biol..* 83, 468–486.

P. Tracqui (1995). From passive diffusion to active cellular migration in mathematical models of tumour invasion. *Acta Biotheoretica.* 43, 443–464.